JACS
JOURNAL OF THE AMERICAN CHEMICAL SOCIETY
Communication
pubs.acs.org/JACS

On-Demand Self-Assembly of Supported Membranes Using Sacrificial, Anhydrobiotic Sugar Coats

Thomas E. Wilkop,*[,†] Jeremy Sanborn,[‡] Ann E. Oliver,[†] Joshua M. Hanson,[§] and Atul N. Parikh*[,†,‡,§,¶]

[†]Department of Biomedical Engineering, University of California, Davis, California, 95616 United States
[‡]Applied Science Graduate Group, University of California, Davis, California, 95616 United States
[§]Biophysics Graduate Group, University of California, Davis, California, 95616 United States
[¶]Department of Chemical Engineering & Materials Science, University of California, Davis, California, 95616 United States

Supporting Information

ABSTRACT: Borrowing principles of anhydrobiosis, we have developed a technique for self-assembling proteolipid-supported membranes on demand—simply by adding water. Intact lipid- and proteolipid vesicles dispersed in aqueous solutions of anhydrobiotic trehalose are vitrified on arbitrary substrates, producing glassy coats encapsulating biomolecules. Previous efforts establish that these carbohydrate coats arrest molecular mobilities and preserve native conformations and aggregative states of the embedded biomolecules, thereby enabling long-term storage. Subsequent rehydration, even after an extended period of time (e.g., weeks), devitrifies sugar—releasing the cargo and unmasking the substrate surface—thus triggering substrate-mediated vesicle fusion in real time, producing supported membranes. Using this method, arrays of membranes, including those functionalized with membrane proteins, can be readily produced *in situ* by spatially addressing vitrification using common patterning tools—useful for multiplexed or stochastic sensing and assaying of target interactions with the fluid and functional membrane surface.

Anhydrobiosis[1] is an evolutionarily conserved property among many organisms (e.g., nematodes, rotifers, and tardigrades), allowing them to survive extreme dehydration for extended periods of time spanning decades to even centuries. Mechanisms by which these organisms tolerate dehydration share a common feature: peculiar biochemical adaptation involving synthesis of large quantities (20−50% of dry weight of the organism itself) of small, nonreducing disaccharide sugars (e.g., sucrose and trehalose),[1b] which vitrify both intra- and extracellularly under drying conditions. Mechanistically, how sugars confer protection to dehydrating biomolecules involves multiple factors:[2] (1) the ability of sugars to substitute for the hydrogen bonds between water and polar residues in labile biomolecules and their assemblies (water replacement hypothesis);[2a] (2) the formation of a trehalose cage, which traps slow-moving water around biomolecules (water entrapment mechanism);[2b] and (3) the formation of a mechanically protective glass by vitrification of sugar, which arrests long-range molecular mobilities (mechanical entrapment scenario).[2c,d] Upon availability of water, dissolution of sugar abandons the quiescent state, reanimating the biomolecules and restoring normal biological functions.

Drawing inspiration from these mechanisms, room-temperature strategies have been previously developed for long-term preservation of biomolecules (e.g., membranes, proteins, and cells) in the dehydrated state.[1b,3] Here, we demonstrate that synthetic surfaces coated with trehalose layers loaded with lipid vesicles (and protein) provide a protective reservoir and a "sacrificial" surface: in the dry "dessication-tolerant" state, the vitrified trehalose coat suspends and preserves the encapsulated cargo. Subsequent introduction of water, even after an extended period of time (e.g., weeks) at the point of application, devitrifies the trehalose—freeing the trapped vesicles (and protein) and unmasking the substrate—thereby triggering an interaction between the freed components (Figure 1). This in turn triggers substrate-induced vesicle fusion, with the unmasked surface (and membrane protein insertion) producing supported membranes.[4] These supported membranes are powerful tools[5] for (1) fundamental biophysical analyses of cellular surfaces;[5a−c] (2) design of protein-resistant surfaces;[5d] and (3) design of membrane-based biosensors for detection of analytes that bind to membrane targets.[5e,f] Their practical utility, however, has been hampered because of a need to maintain them under water, which is cumbersome for long-term storage and transportability, critical for routine or large-scale deployment.[4a] Any exposure to air, or passage through an air−water interface, readily disrupts the supported membrane, causing delamination and loss of structural integrity.[4a] Previously, preformed supported membranes have been rendered air-stable[6] by a variety of methods. Key approaches that have proved successful include linking of the exposed bilayer surface with a close-packed layer of proteins;[6c] incorporation of poly(ethylene glycol)-conjugated lipopolymers;[6a] spin-coating of multilayered films;[6h] or sandwiching of lipid bilayers between carbohydrate, (e.g., sucrose or trehalose) layers.[6d] The anhydrobic membrane concept advanced here simultaneously protects both the biomolecular cargo and the synthetic surface while enabling the *on-demand* production of supported membranes.

We first demonstrate the production of a spatial pattern of single-component phospholipid bilayers. Aliquots of 50−100

Received: October 23, 2013
Published: December 23, 2013

   dx.doi.org/10.1021/ja410866w | *J. Am. Chem. Soc.* 2014, 136, 60−63

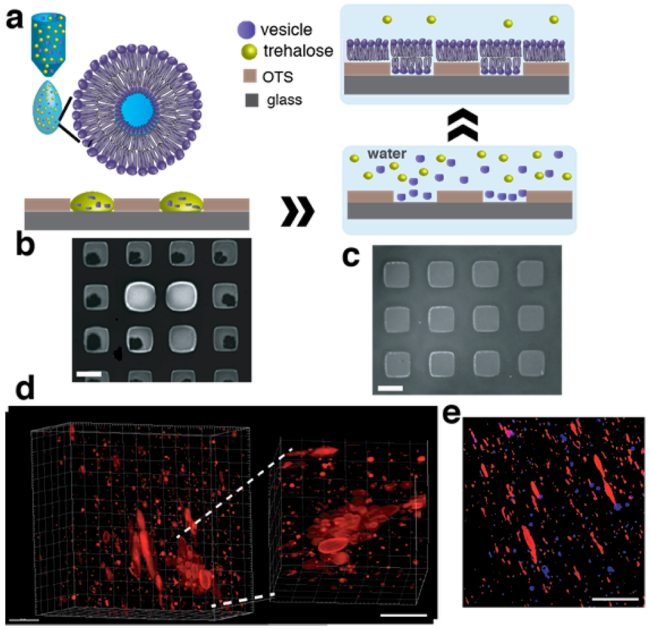

Figure 1. On-demand self-assembly of supported membranes using sacrificial trehalose. (a) Schematic of the method. Vesicle-encapsulating previtrified trehalose coat, upon hydration, releases the cargo which can recognize the unmasked substrate, forming supported membranes. (b,c) Representative epifluorescence micrographs of a pattern of POPC vesicle-embedding arrays of trehalose coats in their vitrified (b) and devitrified (c) states. (d) 3D reconstruction of confocal fluorescence images, showing Texas Red (TR-DHPE)-labeled POPC GUVs encapsulated in vitrified trehalose. Scale bar, 10 μm. (e) False-color composite image, showing the identical region prior to (red) and subsequent to (blue) hydration, revealing the restoration of the spherical shape. Scale bar, 20 μm.

mM trehalose solution (Figure S1) containing preformed small unilamellar vesicles (SUVs) of POPC doped with 1 mol% fluorescent lipid conjugate (TR-DHPE) are deposited on glass slides previously derivatized with spatial patterns of *n*-octadecyltrichlorosilane (OTS) (Supporting Information (SI), Methods). Solution recedes away from the hydrophobic regions, vitrifying (within seconds) on hydrophilic elements of the pattern, which upon further drying forms a spatial array of trehalose coats. Depending upon the deposition method used, patterns of SUV-laden, vitrified trehalose films of hundreds of nanometers to micrometer thicknesses are readily obtained (Figure 1b). Under dry conditions, these patterns remain unperturbed for extended periods of time (several weeks). Subsequent addition of water, even after an extended period (weeks), readily devitrifies the sugar layer, freeing the encapsulated vesicles and baring the underlying substrate. Freed vesicles diffuse, rupture, and fuse with the unmasked surface, producing patterns of single lipid monolayers on OTS-covered regions and bilayers on hydrophilic regions of the substrate surface (Figures 1, S2, and S3).[4d] A combination of epifluorescence microscopy (Figure 1c) and imaging ellipsometry (data not shown) confirms that the physical properties of the resultant lipid bilayer—including uniform surface topography, long-range lateral fluidity (determined using fluorescence recovery after photobleaching (FRAP), D = 2.0−4.0 ± 0.2 μm^2/s, immobile fraction, 5−10%, n = 3; Figure S2), and 3−4 nm thickness—are all in agreement with those of membrane patterns derived by the conventional vesicle fusion method on amphiphilic (hydrophilic/hydrophobic) patterned surfaces.[4d]

What is the fate of vesicles in vitrified trehalose layers? Although trehalose protects the membrane against drying-induced phase transition and vesicle aggregation or fusion,[1b,2e] rapid vitrification of trehalose must introduce osmotic stress on the encapsulated vesicle.[1a] Consequently, intravesicular water can be expected to efflux, changing the surface area to volume ratio, creating conditions for large-scale deformations.[7] To assess the state of the vesicles in vitrified trehalose layers, we carried out independent control experiments. *First,* comparing vesicular sizes of aqueous dispersions derived by rehydrating vitrified trehalose layers with those prior to vitrification by dynamic light scattering confirms that little or no change occurs (Figure S4). *Second,* confocal fluorescence microscopy reveals patchy fluorescence, indicating that the osmotically deflating vesicles do not fuse with the glass slide during vitrification or prior to devitrification (Figure S5). *Third,* to enable direct visualization, we imaged the fate of giant unilamellar vesicles (GUVs, ∼25 μm diameter) trapped in vitrifying trehalose. These results reveal that, although GUVs display significant deformation in vitrified trehalose layers, they do not abandon the vesicular topology (Figure 1d). Moreover, upon devitrification of the trehalose layer, water equilibrates across the vesicular boundary, restoring the original spherical shape (Video S1). Taken together, the three lines of evidence above confirm nondestructive encapsulation of intact lipid vesicles in vitrified trehalose layers.

A powerful feature of our bilayer formation by vesicle fusion on demand is that it allows us to initiate and monitor interactions between reactants (e.g., surface lipids and/or embedded cargo) that are either maintained in separate vesicle populations in the vitrified state or delivered on site during devitrification and bilayer formation.[8] To illustrate these capabilities, we carried out three different classes of experiments.

First, we carried out a lipid-mixing assay. Here, we hydrated vitrified trehalose layers containing primary POPC vesicles (doped with Oregon Green-labeled probe lipid, OG-DHPE) using an aqueous suspension containing identically prepared secondary POPC vesicles doped with TR-DHPE. The two probes interact through Förster resonance energy transfer (FRET): when in Förster proximity (∼5 nm), the emission of OG (a donor) becomes quenched.[9] Companion dynamic light scattering data confirm that, when devitrified in bulk, no noticeable fusion occurs prior to supported bilayer formation (Figures S4 and S5). Epifluorescence images of the supported bilayers so formed strikingly display only red fluorescence (Figure 2a), even when both probes are excited, consistent with the presence of FRET. Extensive FRET (apparent FRET efficiency, E = 0.57; see SI for details) in our data indicates that the lipid content of both populations of vesicles becomes integrated in the resultant, contiguous membrane as a well-mixed, single bilayer, which was confirmed by optical ellipsometry (data not shown). Moreover, FRAP measurements reveal that both probes display long-range fluidity within the contiguous bilayer medium ($D_{\text{OG-DHPE}}$, 1.5 ± 0.2 μm^2/s, immobile fraction, 7−10%; $D_{\text{TR-DHPE}}$, 1.1 ± 0.1 μm^2/s, immobile fraction, 7−10%, n = 3). The FRET between mixed probes in the supported bilayer is further confirmed when the TR-DHPE is selectively photobleached using an intense illumination, when the emission due to OG-DHPE becomes

dx.doi.org/10.1021/ja410866w | J. Am. Chem. Soc. 2014, 136, 60−63

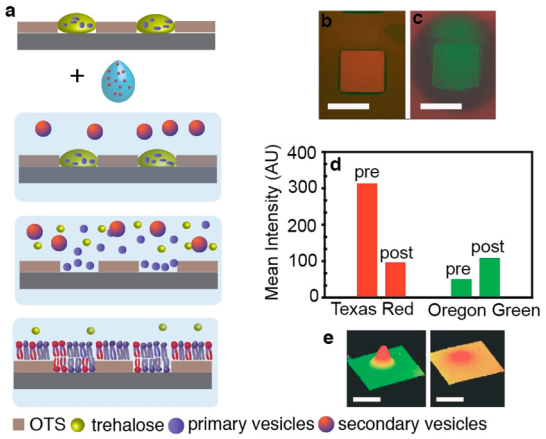

Figure 2. Applications of the membrane on-demand concept. (a) Schematic of lipid mixing, originating from fusion of copopulation of SUVs: one released from the devitrifying trehalose and the second delivered through the devitrification medium. (b,c) Two-color composite fluorescence micrographs (red and green channels) revealing (b) predominantly red fluorescence due to the TR probe and (c) unmasking of the donor (OG) emission by photobleaching the acceptor (TR). Scale bar, 250 μm. (d) Intensity histograms, before and after photobleaching, from which the apparent FRET efficiency is estimated to be E = 0.57. (e) Inverted intensity profiles of a photobleached spot (70 μm diameter) in the TR channel, (left) directly after bleaching and (right) after 20 min recovery. Scale bar, 40 μm.

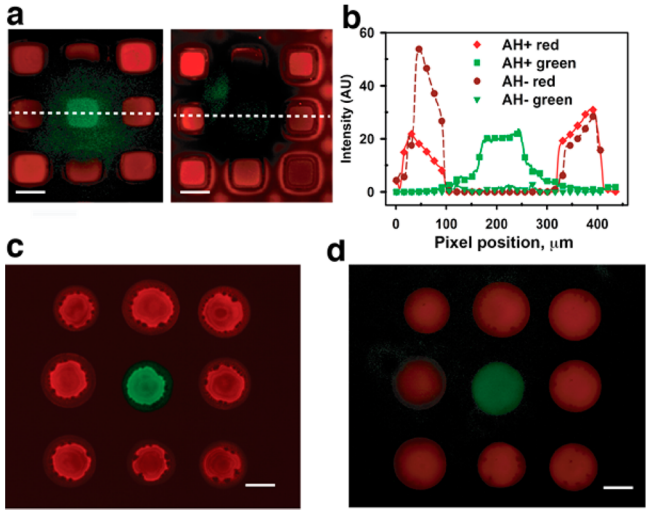

Figure 3. Incorporation of α-hemolysin. (a) Two-color composite fluorescence images of supported bilayers formed by devitrification of α-hemolysin containing POPC bilayers (TR-DHPE-stained) after fluorescence immunoassay with primary and FITC-labeled (green), secondary antibody: (left) after TR photobleaching, which lifts the interfering FRET, and (right) for identically treated negative control sample devoid of α-hemolysin. (b) Comparison of the line profiles of the fluorescence intensities in the red and green channels for TR-DHPE-stained POPC bilayers containing α-hemolysin (AH+) and devoid of the channel protein (AH−), revealing strong antibody binding in the AH+ sample alone. Scale bars, 250 μm. (c,d) Formation of membrane microarrays. Two-color composite fluorescence images of differently stained POPC arrays obtained by devitrifying trehalose: (c) as-deposited dry and (d) after hydration. Scale bars, 300 μm.

apparent (Figure 2b) because of the lifting of the FRET between the probes.

Second, we carried out a ligand-binding assay by hydrating vitrified trehalose coats, which embed cholera toxin (CTxB)-loaded POPC vesicles, using a suspension of secondary POPC vesicles, which present the binding partner, GM1 ganglioside (3 mol%), at the membrane surface (Figure S6). These results reveal that the release of CTxB and presentation of GM1 trigger the binding reaction (see SI).

Third, we carried out a Ca^{2+}-mediated fusion assay (Figure S7) in which a copopulation of vesicles, one containing calcein complexed with cobalt and the other containing EDTA, was seen to remain unreactive in the vitrified state. Upon hydration, the fusion of the two vesicles cobalt complexes with the EDTA freeing the calcein, which in turn increases the fluorescence due to calcein.

To explore whether membrane receptors can be integrated within the rehydrated membrane patterns, we carried out a proof-of-principle experiment using vesicles containing α-hemolysin, a model transmembrane pore-forming protein.[10] Staphylococcal α-hemolysin (αHL), a 33.2 kDa, water-soluble protein, is a member of the class of cytolytic toxins, which convert into a pore-forming homo-oligomer upon insertion into an amphiphilic membrane environment. Simple incubation of αHL monomers with lipid suspension in trehalose solution readily produces proteoliposomes containing a heptameric protein pore.[10b] Vitrifying a trehalose suspension of these proteoliposomes on OTS-patterned substrates (see above) then produces sacrificial coats indistinguishable from those obtained for pure lipid vesicles. Subsequent rehydration of the vitrified trehalose spontaneously produces proteolipid bilayers, incorporating pore-protein, as revealed by monitoring the binding by a pair of highly specific capture-and-probe antibodies (Figure 3a,b).

The generality and flexibility of our membrane on-demand method promise ready adaptation for a variety of applications. For example, in conjunction with spatially addressable deposition methods,[6e,11] such as noncontact[11a] or quill-pin printing[6e] and dip pen nanolithography,[11b] high-density membrane microarrays can be produced on demand that might prove useful for high-throughput drug screening of membrane targets (e.g., GPCRs)[5g] and for parallel and stochastic sensing.[5e] To test for this potential, we used quill-pin printing to deposit vesicle-laden droplets of 50 mM trehalose solution in a spatially directed manner directly on glass. Subsequent rehydration yielded arrays consisting of independent fluid membrane elements (Figure 3c,d). Moreover, real-time exposure of the topochemical character of the substrate upon trehalose devitrification should also enable real-time studies of membrane molecular reorganization in a curvature-dependent manner.[12] Additionally, trehalose coats may also enable activation of cargo consisting of cell-free protein expression extracts[13] together with vesicles, enabling on-site, on-demand production of membrane proteins in synthetic systems. These efforts are currently in progress in our laboratory.

■ ASSOCIATED CONTENT

Ⓢ Supporting Information

Experimental methods, supporting data, supplementary discussion, and Video S1. This material is available free of charge via the Internet at http://pubs.acs.org.

dx.doi.org/10.1021/ja410866w | J. Am. Chem. Soc. 2014, 136, 60−63

AUTHOR INFORMATION

Corresponding Authors

tewilkop@ucdavis.edu
anparikh@ucdavis.edu

Notes

The authors declare no competing financial interest.

ACKNOWLEDGMENTS

We thank A. Revzin and D. Patel for help with the microarrayer. This work was supported by the U.S. Department of Energy, Office of Science, Basic Energy Sciences, under Award # DE-FG02-04ER46173. T.E.W. acknowledges support from University of California, Davis through the Partner Opportunities Program.

REFERENCES

(1) (a) Crowe, J. H.; Hoekstra, F. A.; Crowe, L. M. *Annu. Rev. Physiol.* **1992**, *54*, 579−599. (b) Crowe, L. M. *Comp. Biochem. Physiol. a—Mol. Integrat. Physiol.* **2002**, *131*, 505−513.

(2) (a) Crowe, J. H.; Crowe, L. M.; Chapman, D. *Science* **1984**, *223*, 701−703. (b) Belton, P. S.; Gil, A. M. *Biopolymers* **1994**, *34*, 957−961. (c) Green, J. L.; Angell, C. A. *J. Phys. Chem.* **1989**, *93*, 2880−2882. (d) Fedorov, M. V.; Goodman, J. M.; Nerukh, D.; Schumm, S. *Phys. Chem. Chem. Phys.* **2011**, *13*, 2294−2299. (e) Koster, K. L.; Lei, Y. P.; Anderson, M.; Martin, S.; Bryant, G. *Biophys. J.* **2000**, *78*, 1932−1946. (f) Corradini, D.; Strekalova, E. G.; Stanley, H. E.; Gallo, P. *Scientific Reports* **2013**, *3*, 1−10. (g) Cordone, L.; Cottone, G.; Giuffrida, S. *Journal of Physics-Condensed Matter* **2007**, 19.

(3) (a) Eroglu, A.; Russo, M. J.; Bieganski, R.; Fowler, A.; Cheley, S.; Bayley, H.; Toner, M. *Nat. Biotechnol.* **2000**, *18*, 163−167. (b) Guo, N.; Puhlev, I.; Brown, D. R.; Mansbridge, J.; Levine, F. *Nat. Biotechnol.* **2000**, *18*, 168−171.

(4) (a) Cremer, P. S.; Castellana, E. T. *Surf. Sci. Rep.* **2006**, *61*, 429−444. (b) Sackmann, E. *Science* **1996**, *271*, 43−48. (c) Tamm, L. K.; McConnell, H. M. *Biophys. J.* **1985**, *47*, 105−113. (d) Howland, M. C.; Sapuri-Butti, A. R.; Dixit, S. S.; Dattelbaum, A. M.; Shreve, A. P.; Parikh, A. N. *J. Am. Chem. Soc.* **2005**, *127*, 6752−6765.

(5) (a) Grakoui, A.; Bromley, S. K.; Sumen, C.; Davis, M. M.; Shaw, A. S.; Allen, P. M.; Dustin, M. L. *Science* **1999**, *285*, 221−227. (b) Brian, A. A.; McConnell, H. M. *Proc. Natl. Acad. Sci. U.S.A.—Biol. Sci.* **1984**, *81*, 6159−6163. (c) Mossman, K. D.; Campi, G.; Groves, J. T.; Dustin, M. L. *Science* **2005**, *310*, 1191−1193. (d) Andersson, A. S.; Glasmastar, K.; Sutherland, D.; Lidberg, U.; Kasemo, B. *J. Biomed. Mater. Res., Part A* **2003**, *64A*, 622−629. (e) Bayley, H.; Cremer, P. S. *Nature* **2001**, *413*, 226−230. (f) Cornell, B. A.; BraachMaksvytis, V. L. B.; King, L. G.; Osman, P. D. J.; Raguse, B.; Wieczorek, L.; Pace, R. J. *Nature* **1997**, *387*, 580−583. (g) Groves, J. T. *Curr. Opin. Drug Discovery Dev.* **2002**, *5*, 606−612.

(6) (a) Albertorio, F.; Diaz, A. J.; Yang, T. L.; Chapa, V. A.; Kataoka, S.; Castellana, E. T.; Cremer, P. S. *Langmuir* **2005**, *21*, 7476−7482. (b) Deng, Y.; Wang, Y.; Holtz, B.; Li, J.; Traaseth, N.; Veglia, G.; Stottrup, B. J.; Elde, R.; Pei, D.; Guo, A.; Zhu, X. Y. *J. Am. Chem. Soc.* **2008**, *130*, 6267−6271. (c) Holden, M. A.; Jung, S. Y.; Yang, T. L.; Castellana, E. T.; Cremer, P. S. *J. Am. Chem. Soc.* **2004**, *126*, 6512−6513. (d) Oliver, A. E.; Kendall, E. L.; Howland, M. C.; Sanii, B.; Shreve, A. P.; Parikh, A. N. *Lab Chip* **2010**, *10*, 3427−3427. (e) Fang, Y.; Frutos, A. G.; Lahiri, J. *J. Am. Chem. Soc.* **2002**, *124*, 2394−2395. (f) Fang, Y.; Peng, J. L.; Ferrie, A. M.; Burkhalter, R. S. *Anal. Chem.* **2006**, *78*, 149−155. (g) Gupta, G.; Lyer, S.; Leasure, K.; Virdone, N.; Dattelbaum, A. M.; Atanassov, P. B.; Lopez, G. P. *ACS Nano* **2013**, *7*, 5300−5307. (h) Simonsen, A. C.; Bagatolli, L. A. *Langmuir* **2004**, *20*, 9720−9728.

(7) Mui, B. L. S.; Cullis, P. R.; Evans, E. A.; Madden, T. D. *Biophys. J.* **1993**, *64*, 443−453.

(8) (a) Chan, Y. H. M.; Lenz, P.; Boxer, S. G. *Proc. Natl. Acad. Sci. U.S.A.* **2007**, *104*, 18913−18918. (b) Chiu, D. T.; Wilson, C. F.; Ryttsen, F.; Stromberg, A.; Farre, C.; Karlsson, A.; Nordholm, S.; Gaggar, A.; Modi, B. P.; Moscho, A.; Garza-Lopez, R. A.; Orwar, O.; Zare, R. N. *Science* **1999**, *283*, 1892−1895. (c) Christensen, S. M.; Bolinger, P. Y.; Hatzakis, N. S.; Mortensen, M. W.; Stamou, D. *Nat. Nanotech.* **2012**, *7*, 51−55.

(9) Stryer, L. *Annu. Rev. Biochem.* **1978**, *47*, 819−846.

(10) (a) Braha, O.; Walker, B.; Cheley, S.; Kasianowicz, J. J.; Song, L. Z.; Gouaux, J. E.; Bayley, H. *Chem. Biol.* **1997**, *4*, 497−505. (b) Menestrina, G.; Bashford, C. L.; Pasternak, C. A. *Toxicon* **1990**, *28*, 477−491.

(11) (a) Kaufmann, S.; Sobek, J.; Textor, M.; Reimhult, E. *Lab Chip* **2011**, *11*, 2403−2410. (b) Lenhert, S.; Brinkmann, F.; Laue, T.; Walheim, S.; Vannahme, C.; Klinkhammer, S.; Xu, M.; Sekula, S.; Mappes, T.; Schimmel, T.; Fuchs, H. *Nat. Nanotech.* **2010**, *5*, 275−279.

(12) (a) Parthasarathy, R.; Yu, C. H.; Groves, J. T. *Langmuir* **2006**, *22*, 5095−5099. (b) Tian, A.; Baumgart, T. *Biophys. J.* **2009**, *96*, 2676−2688. (c) Sanii, B.; Smith, A. M.; Butti, R.; Brozell, A. M.; Parikh, A. N. *Nano Lett.* **2008**, *8*, 866−871.

(13) (a) Kai, L.; Doetsch, V.; Kaldenhoff, R.; Bernhard, F. *PLoS One* **2013**, 8. (b) Noireaux, V.; Libchaber, A. *Proc. Natl. Acad. Sci. U.S.A.* **2004**, *101*, 17669−17674.